Transcriptomic Phases of Periodontitis Lesions Using the Nonhuman Primate Model

Jeffrey Ebersole (jeffrey.ebersole@unlv.edu)
University of Nevada, Las Vegas
Radhakrishnan Nagarajan
Marshfield Research Foundation
Sreenatha Kirakodu
University of Kentucky
Octavio A. Gonzalez
University of Kentucky

Research Article

Keywords: Transcriptomic Phases, Nonhuman Primate Model, Periodontitis Lesions, Periodontal diseases

Posted Date: February 10th, 2021

DOI: https://doi.org/10.21203/rs.3.rs-180948/v1

Version of Record: A version of this preprint was published at Scientific Reports on April 29th, 2021. See the published version at https://doi.org/10.1038/s41598-021-88803-6.

Transcriptomic Phases of Periodontitis Lesions using the Nonhuman Primate Model

Jeffrey L. Ebersole[1,#a,*], Radhakrishnan Nagarajan[2,#b], Sreenatha Kirakodu[3], and Octavio A. Gonzalez[3,4]

[1]Department of Biomedical Sciences, School of Dental Medicine, University of Nevada Las Vegas, USA

[2]Center for Oral and Systemic Disease, Marshfield Research Foundation, Marshfield, WI, USA

[3]Center for Oral Health Research College of Dentistry, University of Kentucky, Lexington, KY, USA

[4]Division of Periodontology, University of Kentucky, Lexington, KY, USA

[#a]Previous address: Center for Oral Health Research College of Dentistry, University of Kentucky, Lexington, KY, USA

[#b]Previous address: Division of Biomedical Informatics, College of Medicine, University of Kentucky, Lexington, KY, USA

*Corresponding author: Dr. Jeffrey L. Ebersole
Professor and Associate Dean for Research
School of Dental Medicine, B221
University of Nevada Las Vegas
1001 Shadow Lane
Las Vegas, NV 89106
Jeffrey.ebersole@unlv.edu

ABSTRACT

We used a nonhuman primate model of ligature-induced periodontitis to identify patterns of gingival transcriptomic changes demarcating phases of periodontitis lesions (initiation, progression, resolution). 18 adult *Mulatta macaca* (12-22 years) had ligatures placed (premolar, 1st molar teeth) in all 4 quadrants. Gingival tissue samples were obtained (baseline, 2 weeks, 1 and 3 months during periodontitis and at 5 months resolution). Gene expression was analyzed by microarray [Rhesus Gene 1.0 ST Array (Affymetrix)]. Compared to baseline, a large array of genes were significantly altered at initiation (n=6049), early progression (n=4893), and late progression (n=5078) of disease, with the preponderance being up-regulated. Additionally, 1918 genes were altered in expression with disease resolution, skewed towards down-regulation. Assessment of the genes demonstrated specific profiles of epithelial, bone/connective tissue, apoptosis/autophagy, metabolism, regulatory, immune, and inflammatory responses that were related to health, stages of disease, and tissues with resolved lesions. Unique transcriptomic profiles occured during the kinetics of the periodontitis lesion exacerbation and remission. We delineated phase specific gene expression profiles of the disease lesion. Detection of these gene products in gingival crevicular fluid samples from human disease may contribute to a better understanding of the biological dynamics of the disease to improve patient management.

Introduction

Periodontal diseases are chronic dysregulated responses to dysbiotic microbiomes [1-3]. However, the literature is sparse regarding the earliest changes that occur in the local microbiome at sites that will transition from health to periodontal lesions. Furthermore, the disease is expressed temporally as exacerbations and remissions with the frequency and magnitude of the episodes explaining the variation in disease extent/severity across the population [4,5]. This episodic disease can occur at one or multiple sites sequentially or concomitantly, and appears to occur with greater incidence at sites that have already demonstrated a previous disease process [6-8].

A challenge in the field is that sampling of humans for the comprehensive biology of the disease process remains somewhat problematic for detailing the dynamics of an episodic disease. The experimental designs are generally limited to a point-in-time with clinical definition of health or disease at that point, and thus not providing an accurate representation of the differences in phases of initiation, progression, stabilization, or resolution of the disease lesion at a particular site. Additionally, while investigations of periodontitis in rodents and rabbits [9,10] clearly can provide useful information regarding the underlying biology of local and systemic host responses, the autochthonous complex microbiomes are completely different in these species versus humans, and the major oral pathogens in human disease have no tropism for colonizing rodents and rabbits [11-13]. Thus, we and others have employed a nonhuman primate model of periodontal disease over the last nearly 40 years. It has been shown that the microbiology, immunology, and clinical expression of periodontitis are quite similar in humans and nonhuman primates, including naturally-occurring disease that increases with aging [14-16].

We have also recently reported a familial relationship of periodontitis susceptibility and resistance in multigenerational matrilines of *Macaca mulatta* [14] consistent with some heritability/genetic contribution to the disease, as has been described in humans [17-19].

Thus, this report describes longitudinal studies of biological processes of periodontitis using a nonhuman primate model of ligature-induced disease. Gene expression profiles were determined in gingival tissues with health and during initiation, progression, and resolution of periodontitis, reflecting the episodic nature of the disease in humans. The hypothesis tested was that there would be unique gene expression profiles that discriminate phases of periodontitis. The findings would shed some light into the temporal nature of changes in biological factors/pathways through the disease process. This would provide the potential for identifying targeted biomolecules that could be used to better characterize disease sites in humans, and identify differences in the biological characteristics of healthy (never diseased) sites from previously diseased sites that have been successfully treated, as potential biomarkers of future risk for disease.

Results

Dynamics of periodontitis lesions

Fig 1 provides a schematic model of periodontitis as suggested from human studies of exacerbation and remission of clinical features of disease. It is well recognized that periodontitis is generally not expressed until about the 3rd – 4th decade of life, even though the host response system and oral microbiome are interacting during a 30+ year time period prior to disease [20-22]. Existing data support that many or most of the bacteria generally associated with periodontitis are also present in younger individuals, who often demonstrate substantial

gingival inflammation, but do not appear to transition to destructive disease [23-27]. Additionally, numerous reports have suggested a genetic contribution to disease related to gene polymorphisms that would exist from the beginning of life in at-risk individuals [17]. Thus, the "risk microbiome' and "risk genetic predisposition" occur for decades prior to clinical disease expression. At some point within an individual at one or more sites a disease process is initiated. Based upon the biology of how a host reacts to a bacterial challenge, this initial insult would likely last for days or weeks, either resolving rapidly or transiting to progressing disease. It is unknown regarding the temporal linkage of the biological changes with detectable clinical disease, but it would be predicted that this interaction occurs with disease progression over weeks to months based upon rodent and nonhuman primate experimental data [9,10,28]. While once clinical tissue destruction has occurred, it is irreversible, human studies would support that the disease can and does resolve biologically, limiting the extent of destruction [4,29,30]. With a particular disease lesion, this now stabilized site may exist for weeks or even years; however, human studies support that the greatest predictor of formation of a periodontal lesion is past disease at the same site [5,31]. Nevertheless, there is minimal guidance regarding the biology of resolved sites relative to future disease exacerbations. Thus, we implemented a study to examine this temporal nature of the disease process in nonhuman primates, focusing on gingival gene expression profiles to identify unique biologic processes occurring at the different stages of disease.

Fig 2 summarizes the clinical presentation of ligated teeth for bleeding on probing and probing pocket depth. Consistent with previous studies, inflammation and tissue destructive changes occurred rather rapidly following initiation of the challenge (i.e. 0.5 months), and

continued to progress over 1-3 months. Removal of the ligatures after sampling at 3 months resulted in a general clinical resolution of these disease features that approximated the baseline health values.

Gene expression profiles in periodontitis lesions

A detailed examination (**Table 1**) showed a substantial number of genes with significant differences from baseline samples. These included genes that were both up- and down-regulated at ≥1.5-fold with disease initiation and progression. Interestingly, while there was a large number of genes that were significantly different between disease resolution and baseline, only about 400 demonstrated this fold-level of differential expression.

Since a goal was to identify genes that were uniquely expressed at each time point, the plots in **Fig 3** provide the features of expression for subsets of the genes for baseline expression compared to the other time points. As shown, 358, 330, 271, and 80 genes at 0.5, 1, 3 and 5 months, respectively that fulfilled the threshold of $\geq$1.5 difference between baseline and any other time point. Of interest was that during disease these genes were up-regulated, while at resolution the distinctive genes were expressed at a lower-level than baseline. **Fig 4** depicts a similar analysis of gene expression during disease initiation, progression and resolution compared to all other phases. This differential expression showed a limited number of genes (n=20) and (n=24) that were distinct at 0.5 and 1 month, respectively. At 3 months (late progression), 68 genes showed altered expression. As noted with the baseline comparison the primary effects on gene expression with resolution was a profile of significantly decreased expression of genes (n=18) compared to the other time points.

Functional characteristics of gene expression of periodontitis lesions

131 The next step in the process was to identify those genes/pathways that provided unique
132 signatures for baseline healthy tissues, tissues from sites with initiation and progression of
133 disease, and tissue samples from clinically resolved lesions. **Fig 5** summarizes the functional
134 categories of the genes that were altered at each of the phases compared to baseline healthy
135 tissues. Numerous genes related to epithelial cell biology were altered as early as 2 weeks
136 (Initiation) and remained different from health throughout lesion progression and even in
137 resolution tissues. Inflammation genes were overly represented at disease initiation,
138 decreasing in number with disease progression. Additionally, cellular metabolic and regulatory
139 genes were affected rapidly at disease initiation and early progression and decreased in
140 representation in late progression and resolution. Finally, adaptive immune genes were highly
141 represented in early and late disease progression, with many remaining altered even in
142 resolution samples. **Table 2** provides a summary of the gene expression profile functions that
143 were phase-related across health, disease and resolution samples. In healthy tissues, epithelial
144 cell, metabolic, and regulatory genes generally were elevated and down-regulated with disease.
145 In contrast, genes related to adaptive immune responses were expressed at low levels in
146 healthy tissues and increased significantly in prevalence with disease. With disease initiation,
147 inflammatory gene numbers were substantially increased as were changes in additional genes
148 related to epithelial cell functions and integrity of the epithelium. Early progression showed a
149 more limited number of genes that were differentially expressed compared to all other time
150 points, primarily for epithelial cell genes (decreased) and adaptive immune genes (increased).
151 A distinctive gene profile was observed during late progression, with 96% of the phase specific
152 genes associated with adaptive immune responses. Finally, in resolution samples, a low

number of unique differentially expressed genes was observed with expression of primarily inflammation-associated genes remaining elevated.

A listing of genes that specifically hallmarked healthy gingival tissues from the stages of disease or resolved lesions is provided in **Table 3**. Of these 43 genes, those related to epithelial cells, were generally expressed in significantly elevated levels in healthy tissues and decreased with onset of disease. In contrast, cellular metabolism, regulatory, and inflammation/immune genes were increased with disease onset and progression. **Table 3** also provides a similar summary identification of 45 genes that hallmarked disease initiation/early progression of the lesion. These genes were generally up-regulated during these stages of disease and were represented by a broad mix of functions, generally significantly increased over baseline healthy levels. Examination of unique phase specific gene expression profiles during late progression of disease identified 45 altered transcript signals (**Table 3**). These were skewed towards genes related in inflammation and immune responses. As with gene expression at initiation/early progression, these identified genes were increased compared to baseline samples. However, the most prominent markers comprising >50% of the up-regulated genes were associated with immunoglobulin formation and antibody recombination processes of adaptive immune responses. Finally, we identified gene differences (n=33) in baseline healthy sites versus sites that appeared clinically healthy post-resolution of a disease process (**Table 3**). Of note was that a number of these genes were decreased from health with disease and continued at a lower level of expression in the resolution samples, albeit, at levels improved over the disease samples (eg. keratins, LIPM). MUC4 was unique in that it was increased with disease, but increased to even greater levels once the disease had resolved. In contrast, EGR1 was

decreased with disease from health and was down-regulated even more in resolution samples. Additionally, some genes, eg. CD36, PTGS2 genes were decreased only in resolved disease tissues versus health or disease. While not included in the table, an observation was that of the array of Ig genes of adaptive immunity that were significantly elevated in late progression, remained elevated in resolution compared to healthy tissue samples.

Discrimination of gingival tissues in health and disease

We then evaluated the capacity of these subsets of differentially expressed genes to discriminate the various stages of health and disease in the gingival samples. A principal components analysis (**Fig 6**) summarizes the results. These Principal Components accounted for 62% of the variation in the samples derived from the various time points. As noted the baseline healthy samples and disease initiation (0.5 months) samples demonstrated the greatest discrimination. Also, the distribution of resolution samples suggests a subset that overlapped with healthy patterns, and a second subset appeared more similar to the expression profiles for late progression (3 months). Finally, the early progression samples showed some separation from the other disease points, although the individual variation and overlap with both initiation and/or late progression, supported the limited number of unique gene patterns for the 1 month time point.

Classification of phases of periodontitis lesions using gene expression profiles

Finally, using a set of 67 genes, based upon differential expression at one or more of the timepoints, we created a flow chart to determine expression levels of each of these genes related to discriminating the phase of disease (**Fig 7**). From this measure, we determined threshold values for the ratios that were distinctive for the healthy and disease phase samples.

We then determined for each sample, the number of expression values for individual gingival samples that fell above or below the threshold. This resulted in 4 different gene clusters (I-IV) represented by 20, 12, 16 and 18 genes respectively (**Table 4**). Additionally, subgrouping the Cluster I genes into IA and IB with a different threshold (**Table 4**) was effective in differentiating the baseline healthy samples to those tissues with clinically resolved lesions. **Fig 8** provides a summary of the 18 specimens collected at each of the 5 time points. As noted Clusters I-IV identified health from disease with 15/18 health and only 3/18 were misclassified. Cluster II-IV gene response profiles accurately categorized 15/18 samples at disease initiation (2 weeks) and 17/18 samples at the time of late disease progression (3 months). Of interest was using these 3 clusters of responses, the early progressing lesions demonstrated a very mixed pattern of responses with 2 samples classified with health, 4 samples classified with initiation, 9 samples classified with early progression, and 3 classified with late progression specimens. The results suggest that the early progression of the lesion appears to vary biologically across the individual animals in response to the ligature challenge. **Fig 8** also demonstrates the ability of the response profile of genes in Cluster IA and IB to classify what appears to be a different biology of the baseline healthy samples to those from teeth that had lesions that had clinically resolved. Using the adjusted thresholds, 13/18 healthy and 11/18 resolution samples were accurately classified.

Discussion

Critical features of the underlying biological processes that occur during the transition from periodontal health to disease remain elusive. It is clear that accompanying the clinical changes that hallmark this site specific mucosal disease, numerous biomarkers of inflammation

and altered innate and adaptive immune response parameters can be detected in the subgingival sulcus via gingival crevicular fluid [32-35], and even in whole saliva [36-38] reflecting these local changes. While an array of reports using rodent models of disease have attempted to document the various host response components that contribute to the clinical changes, these models are limited by a lack of any similarity to the oral microbiome in human disease and generally use a biased host response assessment focusing on individual or a finite array of factors of interest. Papapanou and colleagues [39-41] have reported a range of studies of human gingival tissue transcriptomes comparing chronic to aggressive disease, and attempting to identify crucial pathways and transcription factors that associate with existing disease. An observation from these data was the extensive heterogeneity in expression of genes in diseased tissues generally attributed to individual variation in host response genetics and the individual's oral microbiome. However, this report describes an additional alternative for the variation in the human transcriptome profiles, that is, the human samples are obtained at a point-in-time and classified by clinical measures that could have occurred weeks/months previously, could reflect ongoing progression, or could be a disease stable site only presenting a history of a disease process. Thus, we employed a monkey model of ligature-induced disease by which we can directly identify initiation, progression, and resolution of periodontal lesions that would be difficult to accomplish in the human disease model.

This experimental model enabled us to identify transcriptomes in the gingival tissues derived from different phases of the disease process. The goal of detailing the transcriptome would be to document arrays of genes with elevated or depressed expression that discriminated healthy tissues, as well as initiation and progression of disease, and finally were

uniquely expressed with disease resolution. As was expected there was a large number of genes that changed in transition from health to disease, including 900-1400 that were significantly different and either increased or decreased with disease. Additionally, there was a large number of genes that were significantly different between healthy and resolved tissues, albeit a rather limited number with substantial fold-differences.

A global transcriptomic analysis revealed a panel of genes that were specifically elevated in healthy tissues, as well as portfolios of genes that showed unique patterns at 0.5 months (initiation), 1 month (early progression), and 3 months (late progression) compared to the other time points. We also noted a panel of genes with levels elevated in resolved lesions compared to baseline or disease phases. In order to drill down more deeply within the transcriptome to identify the genes of interest, we increased the stringency for inclusion in developing these phase specific panels. This approach provided a subset of about 200+ genes that showed differential expression at the phases of disease and healthy tissues. Interestingly, at this increased level of stringency we found 53 genes in resolved tissues that differed from baseline with 59% showing decreased expression. A second step was to explore features of the panels that discriminated disease initiation from other disease phases or resolution. The results demonstrated few genes that differed uniquely between initiation and early progression. Thus, while the clinical parameters increased significantly from 2 weeks (0.5 months) to 1 month, it appears that changes in gene expression occur rapidly and are maintained during this early progression phase of disease. In contrast, we identified 104 genes that identified tissues at late disease progression versus levels in tissue samples during disease initiation with 58% of the expression levels greater in late progression. This suggested the likelihood of some specific

gene profiles whose function may contribute to the continued progression of the disease lesions. Finally, a number of genes (n=55) were decreased in resolved tissues compared to expression during any phase of disease. Most of these represented gene expression levels that were returning back towards baseline levels consistent with the improved clinical parameters.

These findings documented the existence of genes that demonstrated significant differences across the biologic phases of the disease process and enabled the creation of profiles of "phase-specific" genes. The genes elevated in health, but never in diseased tissues were over-represented for biologic pathways of epithelial cell functions, metabolism, and inflammation (Table 2). At the initiation of disease, an array of genes related to biologic functions of epithelial cells, connective tissue, metabolism and inflammation were observed that clearly demonstrated the transition from health to disease. As these gene expression variations represent early disease changes in this human-like disease model, potentially a subset of these gene products could be targeted as early biomarkers of disease in humans, potentially enabling earlier identification and intervention to minimize tissue damage.

The data also explored the determination if a pattern of genes was also relatively specific for what would be considered "early progression" (1 month) in this model related to clear increases in the trajectory of clinical parameters of BOP and PPD. Interestingly, a rather broad variation in expression of the various clusters of genes was noted during early progression. In the nonhuman primate model, extensive studies of clinical measures have demonstrated a general expression of periodontal disease within 1 month post-ligation in nearly all animals although the rate differs for individual animals [42-44]. Also, a portion of the animals demonstrate clinical measures that show minimal increases between 1 and 3 months

(early responders), while a subset of the animals clearly demonstrate a continued progression of disease, reaching maximum PPD at the 3 month time point, which we defined as “late progression”. As such, the gene analysis prediction grouped selected animals at early progression as either initiation, early or late progression, suggesting an extent of biologic variation in the population during the early transition to progressing destructive disease. This type of temporal variability is likely also reflected within the human population based upon clinical measures of gingivitis and progressing periodontitis, albeit little is known regarding the biological differences occurring with this disease transition. In contrast, the gene profiling analysis identified an array of genes with levels that were expressed uniquely at 3 months (late progression) and were able to discriminate this disease phase. These included immune pathways and, of particular note was the large array of gene expression changes related to formation and recombination events for antibody molecules. Moreover, some genes that were increased at 1 month continued to increase to an even greater extent at 3 months, while other members of this late progressing panel were elevated only at this phase of disease. These patterns enabled the identification of a set of 67 genes that could be assembled into 4 clusters and used to classify health and disease phases. Creating thresholds for individual gene expression, the 4 clusters effectively classified the specimens from healthy sites with >80% accuracy and delineated the initiation and late progression samples at 72% and 94% accuracy, respectively.

Finally, the data provided insight into fundamental biologic differences between gingival tissues of periodontal health and clinically normal gingiva at sites where the lesion has resolved. As might be expected, there was a limited number of genes with expression differences

between healthy and resolved gingival tissues representing epithelial biology and inflammatory responses. However, using additional threshold levels for expression of Cluster I genes 75-80% of the healthy versus resolved specimens were categorized accurately. Thus, the gingival tissues do not appear to return to complete biologic health within 60 days of clinical disease resolution. This might suggest that previously diseased sites that have been treated and resolved may appear clinically normal; however, they could remain biologically programmed for a heightened risk of disease related to a subsequent noxious challenge. Similarly a recent clinical study reported that even in well-maintained patients the oral microbiome seems more pathogenic than in healthy control sites without previous history of periodontitis [45]. This finding also supports a new concept related to the recent classification scheme for periodontitis and reinforces the concept that a patient with periodontal disease experience will be always a patient with enhanced periodontal disease risk even after reaching clinically healthy conditions.

This model provided us the capacity to develop algorithms of gene expression that enabled phasing disease and distinguish between resolved and uninvolved healthy sites. Based upon existing data from cross-sectional human gingival transcriptomes [46-49], we can test these gene panels with the human data to potentially enhance the homogeneity of the human specimens for disease phases and resolution and identify with more precision biomarkers that may be useful in management of the human disease. However, utility of this specific gene expression knowledge would be limited for clinical care in humans since routine sampling of gingival tissues for targeted gene expression would not be feasible. Nevertheless, many of these genes would be predicted to result in secreted translated biomolecules that would be expected to be present in the gingival crevicular fluid and could even be detected in saliva to

potentially discriminate health, disease phases, and resolved lesions. Importantly, as shown in **Table 5** many of these biomolecules have already been evaluated and associate with many chronic inflammatory conditions. Based upon this unbiased approach to identification of potential biomarkers, panels of a finite number of gene products could be evaluated in humans to enable a better understanding of molecular mechanisms and development of targeted therapies with more precision.

Methods

Animal model of periodontitis

Rhesus monkeys (*Macaca mulatta*) (n=18; 10 females and 8 males) aged 12-23 years housed at the Caribbean Primate Research Center at Sabana Seca, Puerto Rico [50-52]. The nonhuman primates were typically fed a 20% protein, 5% fat, and 10% fiber commercial monkey diet (diet 8773, Teklad NIB primate diet modified: Harlan Teklad, Madison, WI). The diet was supplemented with fruits and vegetables, and water was provided *ad libitum* in an enclosed corral setting.

All experimental protocols were approved by the Institutional Animal Care and Use Committees (IACUC) of the University of Puerto Rico and University of Kentucky. The methods were carried out in accordance with all relevant regulations for the use of nonhuman primates following ARRIVE guidelines. Anesthetized animals were examined by a single investigator using a Maryland probe on the facial aspect of the teeth, 2 proximal sites per tooth (mesio- and disto-buccal), excluding the canines and 3rd molars. The clinical examination included probing pocket depth (PD), and bleeding on probing (BOP; 0-5 scale) [16]. Periodontal health was defined by mean Pocket Depth (PD) ≤ 3.0 mm and mean Bleeding on Probing (BOP) ≤ 1 (0-5 scale) in a full

mouth examination excluding 3rd molars and canines[53]. Determination of periodontal disease at the sampled site was documented by assessment of the presence of BOP and probing pocket depth of >4 mm as we have described previously.

Ligature-induced periodontitis was induced in each of the animals at 1st premolar and 1st and 2nd molars in all 4 quadrants following a baseline sampling of gingival tissue from a healthy site. Further, clinical evaluation for ligated sites was obtained and a buccal gingival papilla from each animal was taken using a standard gingivectomy technique at 2 weeks (initiation of disease), and 1 month and 3 months (progression of disease). Then, ligatures were removed after sampling at 3 months and samples taken 2 months later (resolution) [28,54,55].

Gingival tissue sample collection and mRNA analysis

Gingival tissue samples of healthy of disease sites were surgically collected as we have described previously providing buccal gingival samples from either healthy or periodontitis-affected tissue from the premolar/molar maxillary region of each animal using a standard gingivectomy technique [56-58]. Samples were maintained frozen at -80°C in RNAlater solution until RNA preparation for microarray analysis. Total RNA was isolated from tissues using TRizol reagent (Invitrogen, Carlsbad, CA, USA). After cleaning with Qiagen RNeasy mini kit (Qiagen, Valencia, CA, USA), all microarray RNA expression analyses were done at the University of Kentucky Microarray facility. Tissue RNA samples were submitted to the UK Microarray Core Facility and RNA quality was assessed with an Agilent 2100 Bioanalyzer (Agilent Technologies, Santa Clara, CA, USA). Reverse transcription of equal amounts of RNA from each sample was

371 performed, followed by hybridization to the GeneChip® Rhesus Gene 1.0 ST Array (Affymetrix,
372 Santa Clara, CA, USA) similar to methods we have described previously [51,59,60].

373 **Data analysis**

374 The expression intensities for genes across the 18 samples were estimated using the
375 Robust Multi-array Average (RMA) algorithm with probe-level quintile normalization, as
376 implemented in the Partek Genomics Suite software version 6.6 (Partek, St. Louis, MO). The
377 different groups were initially compared using one-way ANOVA. For genes that had significant
378 mean differences, two sample t-tests were used to investigate differences. The data has been
379 uploaded into the ArrayExpress data base (www.ebi.ac.uk) under accession number: E-MTAB-
380 1977. A number of Affymetrix probes with unique expression profiles in the samples had not
381 been annotated. For these, we used the Ensembl ID (EMBL-EBI) to extract out the nucleotide
382 base sequence for the probe from the Affymetrix Exon/Gene
383 (http://www.affymetrix.com/analysis/index.affx#1_2) website. This sequence was then
384 searched in Blast (https://blast.ncbi.nlm.nih.gov/Blast.cgi) and the highest percent identity for
385 *M. mulatta* selected.

386 Normalized expression profiles of genes that were differentially expressed at least
387 across one of the time points Baseline, 2 weeks, 1 Month, 3 Months, 5 Months with the
388 remaining time points as background were used as input to Principal component analysis (PCA)
389 [61-63]. The first and second dominant eigen values explained ~62% of the variance in the given
390 data and two-dimensional projection of the gene expression profile revealed inherent
391 clustering of the time points.

Acknowledgements

We thank the University of Kentucky Microarray Core for initial analytic support. The work was supported by USPHS grants GM103538/RR020145 and RR03640 to the Caribbean Primate Research Center. Contributions to this work were JLE and OAG in the development and implementation of the protocol, sample collection, data analysis and interpretation, and preparation of the manuscript, SK for preparation of samples, and RN provided the data management, strategy for analysis, and revision of the manuscript. The authors have no conflict of interests with the contents of this report.

References

1 Lamont, R. J., Koo, H. & Hajishengallis, G. The oral microbiota: dynamic communities and host interactions. *Nat Rev Microbiol* **16**, 745-759, doi:10.1038/s41579-018-0089-x (2018).

2 Ebersole, J. L. *et al.* Age and Periodontal Health - Immunological View. *Current oral health reports* **5**, 229-241 (2018).

3 Ebersole, J. L. *et al.* The periodontal war: microbes and immunity. *Periodontol 2000* **75**, 52-115, doi:10.1111/prd.12222 (2017).

4 Chapple, I. L. C. *et al.* Periodontal health and gingival diseases and conditions on an intact and a reduced periodontium: Consensus report of workgroup 1 of the 2017 World Workshop on the Classification of Periodontal and Peri-Implant Diseases and Conditions. *J Periodontol* **89 Suppl 1**, S74-S84, doi:10.1002/JPER.17-0719 (2018).

5 Armitage, G. C. Learned and unlearned concepts in periodontal diagnostics: a 50-year perspective. *Periodontol 2000* **62**, 20-36, doi:10.1111/prd.12006 (2013).

6 Goodson, J. M. Diagnosis of Periodontitis by Physical Measurement: Interpretation From Episodic Disease Hypothesis. *J Periodontol* **63 Suppl 4S**, 373-382, doi:10.1902/jop.1992.63.4s.373 (1992).

7 Goodson, J. M. Clinical measurements of periodontitis. *J Clin Periodontol* **13**, 446-460, doi:10.1111/j.1600-051x.1986.tb01489.x (1986).

8 Koch, G. G. & Paquette, D. W. Design principles and statistical considerations in periodontal clinical trials. *Annals of periodontology / the American Academy of Periodontology* **2**, 42-63, doi:10.1902/annals.1997.2.1.42 (1997).

9 Graves, D. T., Kang, J., Andriankaja, O., Wada, K. & Rossa, C., Jr. Animal models to study host-bacteria interactions involved in periodontitis. *Frontiers of oral biology* **15**, 117-132, doi:10.1159/000329675 (2012).

10 Oz, H. S. & Puleo, D. A. Animal models for periodontal disease. *Journal of biomedicine & biotechnology* **2011**, 754857, doi:10.1155/2011/754857 (2011).

11 Abusleme, L. *et al.* Oral Microbiome Characterization in Murine Models. *Bio Protoc* **7**, doi:10.21769/BioProtoc.2655 (2017).

12 Hasturk, H., Goguet-Surmenian, E., Blackwood, A., Andry, C. & Kantarci, A. 1-Tetradecanol complex: therapeutic actions in experimental periodontitis. *J Periodontol* **80**, 1103-1113, doi:10.1902/jop.2009.090002 (2009).

13 Hasturk, H. *et al.* Topical H2 antagonist prevents periodontitis in a rabbit model. *Infect Immun* **74**, 2402-2414 (2006).

14 Ebersole, J. L. *et al.* Periodontal disease susceptible matrilines in the Cayo Santiago Macaca mulatta macaques. *J Periodontal Res* **54**, 134-142, doi:10.1111/jre.12610 (2019).

15 Roth, G. S. *et al.* Aging in rhesus monkeys: relevance to human health interventions. *Science* **305**, 1423-1426 (2004).

16 Ebersole, J. L., Steffen, M. J., Gonzalez-Martinez, J. & Novak, M. J. Effects of age and oral disease on systemic inflammatory and immune parameters in nonhuman primates. *Clin Vaccine Immunol* **15**, 1067-1075, doi:CVI.00258-07 [pii] 10.1128/CVI.00258-07 (2008).

17 Nibali, L. *et al.* Heritability of periodontitis: A systematic review of evidence from animal studies. *Arch Oral Biol* **109**, 104592, doi:10.1016/j.archoralbio.2019.104592 (2020).

18 de Coo, A., Quintela, I., Blanco, J., Diz, P. & Carracedo, A. Assessment of genotyping tools applied in genetic susceptibility studies of periodontal disease: A systematic review. *Arch Oral Biol* **92**, 38-50, doi:10.1016/j.archoralbio.2018.04.012 (2018).

19 Munz, M. *et al.* A genome-wide association study identifies nucleotide variants at SIGLEC5 and DEFA1A3 as risk loci for periodontitis. *Human molecular genetics* **26**, 2577-2588, doi:10.1093/hmg/ddx151 (2017).

20 Eke, P. I. *et al.* Risk Indicators for Periodontitis in US Adults: NHANES 2009 to 2012. *J Periodontol* **87**, 1174-1185, doi:10.1902/jop.2016.160013 (2016).

21 Eke, P. I. *et al.* Periodontitis prevalence in adults >/= 65 years of age, in the USA. *Periodontol 2000* **72**, 76-95, doi:10.1111/prd.12145 (2016).

22 Eke, P. I. *et al.* Update on Prevalence of Periodontitis in Adults in the United States: NHANES 2009 - 2012. *J Periodontol*, 1-18, doi:10.1902/jop.2015.140520 (2015).

23 Lifshitz, F., Casavalle, P. L., Bordoni, N., Rodriguez, P. N. & Friedman, S. M. Oral Health in Children with Obesity or Diabetes Mellitus. *Pediatr Endocrinol Rev* **14**, 159-167, doi:10.17458/PER.2016.LCB.Oralhealth (2016).

24 Song, H. J. Periodontal considerations for children. *Dent Clin North Am* **57**, 17-37, doi:10.1016/j.cden.2012.09.009 (2013).

25 Albandar, J. M. Epidemiology and risk factors of periodontal diseases. *Dent Clin North Am* **49**, 517-532, v-vi (2005).

26 Papapanou, P. N. Population studies of microbial ecology in periodontal health and disease. *Annals of periodontology / the American Academy of Periodontology* **7**, 54-61 (2002).

27 Bimstein, E., Ram, D., Irshied, J., Naor, R. & Sela, M. N. Periodontal diseases, caries, and microbial composition of the subgingival plaque in children: a longitudinal study. *ASDC J Dent Child* **69**, 133-137, 123 (2002).

28 Madden, T. E. & Caton, J. G. Animal models for periodontal disease. *Methods in enzymology* **235**, 106-119 (1994).

29 Freire, M. O. & Van Dyke, T. E. Natural resolution of inflammation. *Periodontol 2000* **63**, 149-164, doi:10.1111/prd.12034 (2013).

30 Kantarci, A. & Van Dyke, T. E. Resolution of inflammation in periodontitis. *J Periodontol* **76**, 2168-2174 (2005).

31 Armitage, G. C. & Robertson, P. B. The biology, prevention, diagnosis and treatment of periodontal diseases: scientific advances in the United States. *J Am Dent Assoc* **140 Suppl 1**, 36S-43S (2009).

32 Ebersole, J. L., Singer, R. E., Steffensen, B., Filloon, T. & Kornman, K. S. Inflammatory mediators and immunoglobulins in GCF from healthy, gingivitis and periodontitis sites. *J Periodontal Res* **28**, 543-546 (1993).

33 Sadeghi, R., Sattari, M., Dehghan, F. & Akbari, S. Interleukin-17 and interleukin-23 levels in gingival crevicular fluid of patients with chronic and aggressive periodontitis. *Cent Eur J Immunol* **43**, 76-80, doi:10.5114/ceji.2018.74876 (2018).

34 Bostanci, N. *et al.* Gingival Exudatome Dynamics Implicate Inhibition of the Alternative Complement Pathway in the Protective Action of the C3 Inhibitor Cp40 in Nonhuman Primate Periodontitis. *J Proteome Res* **17**, 3153-3175, doi:10.1021/acs.jproteome.8b00263 (2018).

35 Kinney, J. S. *et al.* Crevicular fluid biomarkers and periodontal disease progression. *J Clin Periodontol* **41**, 113-120, doi:10.1111/jcpe.12194 (2014).

36 Nagarajan, R., Al-Sabbagh, M., Dawson, D., 3rd & Ebersole, J. L. Integrated biomarker profiling of smokers with periodontitis. *J Clin Periodontol* **44**, 238-246, doi:10.1111/jcpe.12659 (2017).

37 Javaid, M. A., Ahmed, A. S., Durand, R. & Tran, S. D. Saliva as a diagnostic tool for oral and systemic diseases. *Journal of oral biology and craniofacial research* **6**, 66-75, doi:10.1016/j.jobcr.2015.08.006 (2016).

38 Salminen, A. *et al.* Salivary biomarkers of bacterial burden, inflammatory response, and tissue destruction in periodontitis. *J Clin Periodontol* **41**, 442-450, doi:10.1111/jcpe.12234 (2014).

39 Sawle, A. D., Kebschull, M., Demmer, R. T. & Papapanou, P. N. Identification of Master Regulator Genes in Human Periodontitis. *J Dent Res* **95**, 1010-1017, doi:10.1177/0022034516653588 (2016).

40 Kebschull, M. *et al.* Gingival tissue transcriptomes identify distinct periodontitis phenotypes. *J Dent Res* **93**, 459-468, doi:10.1177/0022034514527288 (2014).

41 Kebschull, M. *et al.* Molecular differences between chronic and aggressive periodontitis. *J Dent Res* **92**, 1081-1088, doi:10.1177/0022034513506011 (2013).

42 Kornman, K. S., Blodgett, R. F., Brunsvold, M. & Holt, S. C. Effects of topical applications of meclofenamic acid and ibuprofen on bone loss, subgingival microbiota and gingival PMN response in the primate Macaca fascicularis. *J Periodontal Res* **25**, 300-307 (1990).

43 Brecx, M. C., Nalbandian, J., Kornman, K. S. & Robertson, P. B. Morphological studies on periodontal disease in the cynomolgus monkey. III. Electron microscopic observations. *J Periodontal Res* **21**, 137-153 (1986).

44 Persson, G. R. *et al.* Macaca fascicularis as a model in which to assess the safety and efficacy of a vaccine for periodontitis. *Oral Microbiol Immunol* **9**, 104-111 (1994).

45 Lu, H. *et al.* Well-maintained patients with a history of periodontitis still harbor a more dysbiotic microbiome than health. *J Periodontol* **91**, 1584-1594, doi:10.1002/JPER.19-0498 (2020).

46 Jonsson, D. *et al.* Gingival tissue transcriptomes in experimental gingivitis. *J Clin Periodontol* **38**, 599-611, doi:10.1111/j.1600-051X.2011.01719.x (2011).

47 Kebschull, M. & Papapanou, P. N. The use of gene arrays in deciphering the pathobiology of periodontal diseases. *Methods Mol Biol* **666**, 385-393, doi:10.1007/978-1-60761-820-1_24 (2010).

48 Demmer, R. T. *et al.* Transcriptomes in healthy and diseased gingival tissues. *J Periodontol* **79**, 2112-2124, doi:10.1902/jop.2008.080139 (2008).

49 Papapanou, P. N. *et al.* Gene expression signatures in chronic and aggressive periodontitis: a pilot study. *Eur J Oral Sci* **112**, 216-223, doi:10.1111/j.1600-0722.2004.00124.x (2004).

50 Gonzalez, O. A. *et al.* Effects of aging on apoptosis gene expression in oral mucosal tissues. *Apoptosis : an international journal on programmed cell death* **18**, 249-259, doi:10.1007/s10495-013-0806-x (2013).

51 Gonzalez, O. A. *et al.* Apoptotic genes are differentially expressed in aged gingival tissue. *J Dent Res* **90**, 880-886, doi:10.1177/0022034511403744 (2011).

52 Ebersole, J. L. *et al.* Differential gender effects of a reduced-calorie diet on systemic inflammatory and immune parameters in nonhuman primates. *J Periodontal Res* **43**, 500-507, doi:JRE1051 [pii] 10.1111/j.1600-0765.2008.01051.x (2008).

53 Ebersole, J. L. *et al.* Cytokine gene expression profiles during initiation, progression and resolution of periodontitis. *J Clin Periodontol*, doi:10.1111/jcpe.12286 (2014).

54 Schou, S., Holmstrup, P. & Kornman, K. S. Non-human primates used in studies of periodontal disease pathogenesis: a review of the literature. *J Periodontol* **64**, 497-508 (1993).

55 Kirakodu, S., Chen, J., Gonzalez Martinez, J., Gonzalez, O. A. & Ebersole, J. Microbiome Profiles of Ligature-Induced Periodontitis in Nonhuman Primates Across the Lifespan. *Infect Immun*, doi:10.1128/IAI.00067-19 (2019).

56 Gonzalez, O. A. *et al.* Differential Gene Expression Profiles Reflecting Macrophage Polarization in Aging and Periodontitis Gingival Tissues. *Immunological investigations* **44**, 643-664, doi:10.3109/08820139.2015.1070269 (2015).

57 Gonzalez, O. A. *et al.* Comparative analysis of gingival tissue antigen presentation pathways in ageing and periodontitis. *J Clin Periodontol* **41**, 327-339, doi:10.1111/jcpe.12212 (2014).

58 Gonzalez, O. A. *et al.* Effects of aging on apoptosis gene expression in oral mucosal tissues. *Apoptosis* **18**, 249-259, doi:10.1007/s10495-013-0806-x (2013).

59 Meka, A. *et al.* Porphyromonas gingivalis infection-induced tissue and bone transcriptional profiles. *Mol Oral Microbiol* **25**, 61-74, doi:OMI555 [pii] 10.1111/j.2041-1014.2009.00555.x.

60 Gonzalez, O. A. *et al.* Comparative analysis of gingival tissue antigen presentation pathways in ageing and periodontitis. *Journal of clinical periodontology* **41**, 327-339, doi:10.1111/jcpe.12212 (2014).

61 Alter, O., Brown, P. O. & Botstein, D. Singular value decomposition for genome-wide expression data processing and modeling. *Proc Natl Acad Sci U S A* **97**, 10101-10106, doi:10.1073/pnas.97.18.10101 (2000).

62 Jolliffe, I. T. *Principal Component Analysis*. 2 edn, (Springer-Verlag, 2002).

63 Yeung, K. Y. & Ruzzo, W. L. Principal component analysis for clustering gene expression data. *Bioinformatics* **17**, 763-774, doi:10.1093/bioinformatics/17.9.763 (2001).

64 Thullier, P., Huish, O., Pelat, T. & Martin, A. C. The humanness of macaque antibody sequences. *Journal of molecular biology* **396**, 1439-1450, doi:10.1016/j.jmb.2009.12.041 (2010).

Figure Legends

Fig 1: Model of exacerbations and remission of periodontal disease lesions. Graph reflects inherent risk due to genetic predisposition and existing oral microbiome characteristics. Biologic changes occur with initiation and progression of disease the generally presage the clinical changes measured. The model indicates that the biological parameters of disease stabilize and decrease during disease remission and resolution. However, the clinical features of lost epithelial attachment, connective tissue destruction and alveolar bone resorption remain as markers of the previous disease process.

Fig 2: Clinical features of inflammation (bleeding on probing, BOP) and destructive disease (probing pocket depth, PPD) in ligated sites of the nonhuman primates. Ligatures were removed after clinical measures at 3 months, with 5 month samples representing clinical resolution. The points denote the mean values from 18 animals and the vertical brackets enclose 1 SD.

Fig 3: Patterns of gene expression with disease and resolution compared to baseline/health and with each time point of disease or resolution compared to all other time points in the model. Numbers in parentheses denote number of genes within the particular patterns, and whether the patterns denoted up (↑) or down-regulation (↓) of the gene experssion.

Fig 4: Patterns of gene expression with disease and resolution compared all other time points in the model. Numbers in parentheses denote number of genes within the particular patterns, and whether the patterns denoted up (↑) or down-regulation (↓) of the gene expression.

Fig 5: Depiction of the array of genes in various functional categories that differed by $\geq$2-fold at health versus other sampling points. Pie charts denote the proportions of each functional

579 category of genes that comprised the overall number of genes (in parentheses) that were
580 differentially expressed.
581 **Fig 6:** Principal components analysis of the 89 gingival tissue samples using the profile of
582 discriminatory genes identified as disease phase-related. Each point denotes the profile of
583 gene expression for an individual gingival tissue sample collected at baseline (healthy), 0.5
584 months (initiation), 1 month (early progression), 3 months (late progression), and 5 months
585 (resolution).
586 **Fig 7:** Flow of specific gene selection for discriminating health, phases of disease, and
587 resolution.
588 **Fig 8:** Map of response profiles for gene clusters for the 18 samples obtained at each of the
589 timepoints. Red denotes sample demonstrated: Cluster I - >13 genes; Cluster II - >9 genes;
590 Cluster III - >7 genes; Cluster IV - >7 genes with signal greater or less than the threshold cutoff
591 normalized signal (T_c, Table 3). Green denotes sample exhibited fewer genes above or below
592 the T_c. Similar depiction of the distribution of responses to Cluster I genes subgrouped into IA
593 and IB. Red denotes IA - >2 genes and IB - >3 genes above/below the T_c (see Table 3). Total %
594 denotes proportion of the samples that were positive in the gene expression cluster.
595

Table 1: Distribution of altered gene expression in gingival tissues during ligature-induced periodontitis and at disease resolution compared to baseline healthy tissues.

Sample (mo.)	**Stage**	**P-value <0.01**	**Gene Expression Changes (#)**	
		Total #	UP (Fold ≥1.5)	DOWN (Fold ≥1.5)
0.5	Initiation	6049	943	472
1	Early Progression	4893	692	471
3	Late Progression	5078	542	372
5	Resolution	1918	176	221

Table 2: Identification of altered gene expression in gingival tissues, with functional patterns unique to each phase of health, disease and resolution by comparison to gene expression profiles in all other phases of lesion formation and resolution. Fxn denotes functional categorization of genes: Epi – epithelium, Conn –connective tissue, Bone, Meta –metabolic, Regul – regulatory, Inflam – inflammation, Imm – innate immune, Adap – adaptive immune, Auto – autophagy, Apop – apoptosis, Pseudo - pseudogene. Value denote number of genes represented in each category.

		Functional Categorization											
Phase	**Total**	**Epi**	**Meta**	**Regul**	**Inflam**	**Imm**	**Adap**	**Conn**	**Vasc**	**Auto**	**Apop**	**Bone**	**Pseudo**
Health/BL	163	45	21	13	10	13	49	6	2	2	0	0	1
Initiation/2 wks.	70	13	7	8	23	1	3	7	5	0	0	0	0
Early Progression/1 mo.	20	10	0	1	1	0	7	1	0	0	0	0	0
Late Progression/3 mo.	50	0	0	1	1	0	48	0	0	0	0	0	0
Resolution/5 mo.	17	1	1	2	10	0	0	2	1	0	0	0	0

606 **Table 3:** Identification of altered gene expression in gingival tissues: comparing healthy versus
607 diseased gingival tissues (n=43; in all cases levels of gene expression were elevated in healthy
608 tissues); during initiation/early progression of disease (n=45); during late progression of disease
609 (n=46); and comparing baseline healthy tissues to clinically resolved lesions (n=33). Fxn denotes
610 functional categorization of genes: Adap – adaptive immune response , Conn –connective
611 tissue/bone, Epi – epithelium, Imm – immune response, Inflam – inflammation, Metab –
612 metabolic, Regul – regulatory, Auto – autophagy/apoptosis, Sig – cellular signaling, UA –
613 unassigned to any of these functions. The Adap genes are the human ID designation related to
614 antibody nucleotide sequences of the macaque probes. Numerous of the matching macaque
615 sequence Ig gene IDs are delineated in Thulliere et al.[64]

Gene ID	FXN	Ontology
Health versus Disease		
ANAX3	Conn	annexin A3
DRAM1	Conn	DNA damage regulated autophagy modulator 1
MMP1	Conn	matrix metalloproteinase 1
PXDN	Conn	peroxidasin
SERPINE2	Conn	serpin family E member 2
TFPI	Conn	tissue factor pathway inhibitor
ALOXE3	Epi	arachidonate lipoxygenase 3
ALOX12B	Epi	arachidonate 12-lipoxygenase, 12R type
CDSN	Epi	corneodesmosin
CRNN	Epi	cornulin
DSC1	Epi	desmocolin 1
KLK5	Epi	kallikrein related peptidase 5
KRT1	Epi	keratin 1
KRT2B	Epi	keratin, type II cytoskeletal 2 oral-like
LCE3C	Epi	late cornified envelope 3C
NID1	Epi	nidogen 1
ODAM	Epi	odontogenic, ameloblast associated
PRR9	Epi	proline rich 9
RPTN	Epi	repetin
SERPINB13	Epi	serpin family B member 13
SPINK9	Epi	serine peptidase Inhibitor, Kazal Type 9
BPIL2/BPILFC	Imm	bactericidal/permeability increasing protein-like 2
SIRPB1	Imm	signal regulatory proten beta 1
SLAMF6	Imm	SLAM family member 6
WFDC12	Imm	WAP four-disulfide core domain 12
CD177	Inflam	CD177 molecule
CSF3R	Inflam	colony stimulating factor 3 receptor (granulocyte)
CXCL8	Inflam	interleukin 8
CXCL6	Inflam	chemokine (C-X-C motif) ligand 6
GSDMA	Inflam	gasdermin A
HPGD	Inflam	15-hydroxyprostaglandin dehydrogenase
IL36B/IL1F8	Inflam	interleukin 36 beta
SERPINB5	Inflam	serpin family B member 5

TNFRSF19	Inflam	TNF receptor superfamily member 19
AADAC	Metab	arylacetamide deacetylase
AKR1C3	Metab	aldo-keto reductase family 1 member C3
ALAS2	Metab	5'-aminolevulinate synthase 2
ARSF	Metab	arylsulfatase F
ESYT3	Metab	extended Synaptotagmin 3
SERPINA3	Metab	serpin family A member 3
TDH	Metab	L-threonine dehydrogenase (pseudogene)
FAM178B	Regul	family with sequence similarity 178 member B
RNU6-1	Regul	U6 spliceosome
Initiation/Early Progression		
BLK	Adap	BLK proto-oncogene, Src family tyrosine kinase
IGKV1-ACY*02	Adap	immunoglobulin kappa variable 1 ACY*02
IGKV1S14*01	Adap	immunoglobulin kappa variable 1S14*01
IGKV3-ACF*02	Adap	immunoglobulin kappa variable 3 ACF*02
IGLV2S9*01	Adap	immunoglobulin lambda variable 2S-9*01
MZB1	Adap	marginal zone B and B1 cell specific protein
MUC4	Auto	mucin 4, cell surface associated
NAIP	Auto	NLR family apoptosis inhibitory protein
RUBCNL	Auto	rubicon like autophagy enhancer
ACTA2	Epi	actin alpha 2, smooth muscle
ADAM12	Epi	ADAM metallopeptidase domain 12
KRT8	Epi	keratin 8
KRT15	Epi	keratin 15
NID2	Epi	nidogen 2 (osteonidogen)
PLIN2/ADFP	Epi	perilipin 2
COL4A2	Conn	collagen type IV alpha 2
ESM1	Conn	endothelial cell-specific molecule 1
HAS2	Conn	hyaluronan synthase 2
PLAU	Conn	plasminogen activator, urokinase
PLAT	Conn	plasminogen activator, tissue type
ADAMTS9	Metab	ADAM metallopeptidase with thrombospondin type 1 motif 9
CTSL	Metab	cathepsin L
CYP4F3	Metab	cytochrome P450 family 4 subfamily F member 3
NOX4	Metab	NADPH oxidase 4
MTHFS	Metab	methenyltetrahydrofolate synthetase
MSMO1	Metab	methylsterol monooxygenase 1
SLC11A1	Metab	solute carrier family 11 member 1
SULF1	Metab	sulfatase 1
TGM2	Metab	transglutaminase 2 (C polypeptide, protein-glutamine-gamma-glutamyltransferase)
IL1B	Inflam	interleukin 1 beta
MIR223	Inflam	microRNA 223
NLRP12	Inflam	NLR family pyrin domain containing 12
SELL	Inflam	selectin L
TLR2	Imm	toll like receptor 2
TLR4	Imm	toll-like receptor 4

IL33	Imm	Interleukin 33
LILRA2	Imm	leukocyte immunoglobulin like receptor A2
PLAC8	Imm	placenta associated 8
CCDC9	Regul	coiled-coil domain containing 9
GLI3	Regul	GLI family zinc finger 3
HGF	Regul	hepatocyte growth factor
RGS18	Regul	regulator of G protein signaling 18
SFRP4	Regul	secreted frizzled related protein 4
OR6K6	Sig	olfactory receptor family 6 subfamily K member 6
RTP3	Sig	receptor transporter protein 3
VWF	UA	Von Willebrand factor
Late Progression		
IGHG3*02	Adap	immunoglobulin heavy constant gamma 3
IGHM	Adap	immunoglobulin heavy constant mu
IGHV3-49	Adap	immunoglobulin heavy variable 3-49
IGHV3-72	Adap	immunoglobulin heavy variable 3-72
IGHV3-73	Adap	immunoglobulin heavy variable 3-73
IGHV3-AGQ*02	Adap	immunoglobulin heavy variable 3 AGQ*02
IGJ	Adap	joining chain of multimeric IgA and IgM
IGKV1-9	Adap	immunoglobulin kappa variable 1-9
IGKV1-ABV*02	Adap	immunoglobulin kappa variable 1 ABV*02
IGKV1-ACY*02	Adap	immunoglobulin kappa variable 1 ACY*02
IGKV1z	Adap	immunoglobulin kappa variable 1z
IGKV2-ABW*04	Adap	immunoglobulin kappa variable 2 ABW*04
IGKV2S19*01	Adap	immunoglobulin kappa variable 2S19*01
IGKV3-ADU*02	Adap	immunoglobulin kappa variable 3 ADU*02
IGKV4-1	Adap	immunoglobulin kappa variable 4-1
IGLV1-ABB*02	Adap	immunoglobulin lambda variable 1 ABB*02
IGLV1-ACV*02	Adap	immunoglobulin lambda variable 1 ACV*02
IGLV2a	Adap	immunoglobulin lambda variable 2a
IGLV2-ABU*02	Adap	immunoglobulin lambda variable 2 ABU*02
IGLV3-AAV*04	Adap	immunoglobulin lambda variable 3 AAV*04
IGLV5-AAX*02	Adap	immunoglobulin lambda variable 5 AAX*02
IGLV7-46	Adap	immunoglobulin lambda variable 7-46
IGLV8-61	Adap	immunoglobulin lambda variable 8-61
KLHL6	Adap	kelch like family member 6
COL4A2	Conn	collagen type IV alpha 2
KRT24	Epi	keratin, type I cytoskeletal 24-like
THBS1	Epi	thrombospondin 1
BANK1	Imm	B cell scaffold protein with ankyrin repeats 1
FPR3	Imm	formyl peptide receptor 3
GREM1	Imm	gremlin 1, DAN gamily BMP antagonist
LST1	Imm	leukocyte specific transcript 1
SERPINB5	Imm	Serpin family B member 5
TEK	Imm	TEK receptor tyrosine kinase
CD36	Inflam	CD36 molecule (thrombospondin receptor)

CXCR1	Inflam	chemokine (C-X-C motif) receptor 1
PTGS2	Inflam	prostaglandin-endoperoxide synthase 2
TREM1	Inflam	triggering receptor expressed on myeloid cells 1
BCAT1	Metab	branched chain amino acid transaminase 1
DYSF	Metab	dysferlin
KYNU	Metab	kynureninase-like
SLC2A14	Metab	solute carrier family 2 member 14
SLC15A1	Metab	solute carrier family 15 member 2
SNORD116-17	Regul	small nucleolar RNA, C/D box 116-17
TENT5C	Regul	terminal nucelotidyltransferase 5C
ZNF337	Regul	zinc finger protein 337
UTS2B	Sig	urotensin 2B
Health versus Resolution		
IGLV2S9*01	Adap	immunoglobulin lambda variable 2S-9*01
IGHV3-ADR*02	Adap	immunoglobulin heavy variable 3 ADR*02
DRAM1	Conn	DNA damage regulated autophagy modulator 1
ESM1	Conn	endothelial cell-specific molecule 1
TFPI	Conn	tissue factor pathway inhibitor
MMP1	Conn	matrix metalloproteinase 1
PXDN	Conn	peroxidasin
KLK5	Epi	kallikrein related peptidase 5
KRT1	Epi	keratin 1
KRT10	Epi	keratin 10
KRT75	Epi	keratin 75
LCE3C	Epi	late cornified envelope 3C
LIPM	Epi	Lipase Family Member M
ALOX12B	Epi	arachidonate 12-lipoxygenase, 12R type
KRT2B	Epi	keratin, type II cytoskeletal 2 oral-like
NID1	Epi	nidogen 1
ODAM	Epi	odontogenic, ameloblast associated
PRR9	Epi	proline rich 9
SPINK9	Epi	serine peptidase Inhibitor, kazal type 9
CRNN	Epi	cornulin
DSC1	Epi	desmocolin 1
SIRPB1	Imm	signal regulatory proten beta 1
SLAMF6	Imm	SLAM family member 6
WFDC12	Imm	WAP four-disulfide core domain 12
CSF3R	Inflam	colony stimulating factor 3 receptor (granulocyte)
CXCL8	Inflam	interleukin 8
CXCL6	Inflam	chemokine (C-X-C motif) ligand 6
HPGD	Inflam	15-hydroxyprostaglandin dehydrogenase
PTGS2	Inflam	prostaglandin-endoperoxide synthase 2
AKR1C3	Metab	aldo-Keto Reductase Family 1 Member C3
EGR1	Regul	early growth response 1
FOS	Regul	Fos proto-oncogene, AP-1 transcription factor subunit
RNU6-1	Regul	U6 spliceosome

Table 4: Gene clusters used to categorize the gingival samples. The threshold cutoff ratio determined as T_c for the normalized signal.

Gene Cluster							
I	**T_c**	**II**	**T_c**	**III**	**T_c**	**IV**	**T_c**
TNFRSF19	>150	ADAM12	>1200	DYSF	>400	CDSN	>1300
ANAX3	>200	PLAT	>150	KYNU	>80	CEACAM8	>600
SERPINE2	>400	MIR223	>400	SLC2A14	>500	LCE3C	>200
CD177	>425	NOX4	>500	CXCR1	<500	NID2	>1500
CSF3R	<350	BLK	>150	SERPINB5	>500	THBS1	>100
ALOX12B	>300	KRT1	>75	KRT24	>250	COL15A1	>100
KRT2B	>100	MUC4	>800	MZB1	>175	COL4A1	>500
NID1	>50	TLR4	>350	EGR1	>65	SERPINE1	>400
MMP1	>300	HAS2	>225	CD36	>200	TGM2	>1100
PXDN	<125	TEK	>200	PTGS2	>400	HGF	<350
CRNN	>300	CTSL	>350	LST1	>400	TREM1	<750
DSC1	>300	RUBCNL	>150	COL4A2	>300	SELL	>20
DRAM1	>60			GREM1	>450	CLDN10	>200
ESM1	<175			FPR3	>350	SFRP4	>325
TFPI	<1000			MZB1	>1000	SNORD116	>150
SIRPB1	<1300			CYP4F3	>225	TENT5C	>1700
HPGD	>350					BANK1	>150
CXCL8	<200					BCAT1	>75
CXCL6	>100						
SLAMF6	>600						
IA	**T_c**	**IB**	**T_c**				
CSF3R	<350	CRNN	<300				
ALOX12B	>350	DSC1	<300				
KRT2B	>125	DRAM1	<50				
NID1	>35	ESM1	>200				
MMP1	>375	TFPI	<750				
PXDN	>125	SIRPB1	>1300				
		HPGD	<350				
		CXCL8	>250				
		CXCL6	<100				
		SLAMF6	<700				

Table 5: Targeted biomarkers for periodontal lesion phases reported as diagnostic biomarkers for various inflammatory and non-inflammatory diseases.

Cluster	Protein	Fluid	Biologic Linkage
I	ALOX12B	serum/plasma	Diabetes
I	CRNN	serum/plasma	Epithelial-induced stress protein
I	CSF3R	serum/plasma	Cancer related gene
I	CXCL6	serum/plasma/urine/saliva	Antibacterial/neutrophil
I	CXCL8 (IL-8)	serum/plasma/saliva	Pancreatic cancer; breast cancer
I	ESM1	serum/saliva	(Endocan) CVD, PCOS
I	HPGD	serum/plasma/saliva	Cancer
I	MMP1	serum/plasma/saliva	CVD; arthritis
I	NID1	plasma/saliva	Cancer
I	PXDN	serum/plasma/saliva	Fibrosis
I	TFPI	serum/plasma	Coagulation
I	TNFRSF19	serum/plasma	Cancer
I	SERPINE2	serum	Cancer
II	TLR4	serum/plasma/saliva	Arthritis, autoimmunity
II	ADAM12	serum/plasma	Fibrosis; lung disease
II	KRT1	serum/plasma	Cancer
II	MIR223	serum/plasma/saliva	Cancer; CVD
II	MUC4	serum/cyst fluid/saliva	Cancer
II	NOX4	serum/plasma	Inflammation
II	PLAT	serum/plasma/saliva	CVD
II	TEK	serum/plasma	Cancer, autoimmune
II	HAS2	serum/plasma/saliva	Inflammation; arthritis
III	CD36	serum/plasma	Foam cell formation (CVD)
III	KYNU	serum/plasma	Psoriasis
III	GREM1	serum	Inflammation
III	FPR3	serum	COPD
IV	SERPINE1	serum/plasma/saliva	CVD (PAI-1)
IV	CEACAM8	serum/plasma/saliva	Arthritis
IV	HGF	serum/plasma/saliva	Liver disease; cancer
IV	NID2	serum/plasma/saliva	Cancer
IV	SELL	plasma	Alzheimer's; schizophrenia
IV	SFRP4	serum/plasma	Diabetes
IV	THBS1	serum/saliva	Obesity; pregnancy
IV	TREM1	serum/saliva	Inflammatory bowel disease

Figures

Figure 1

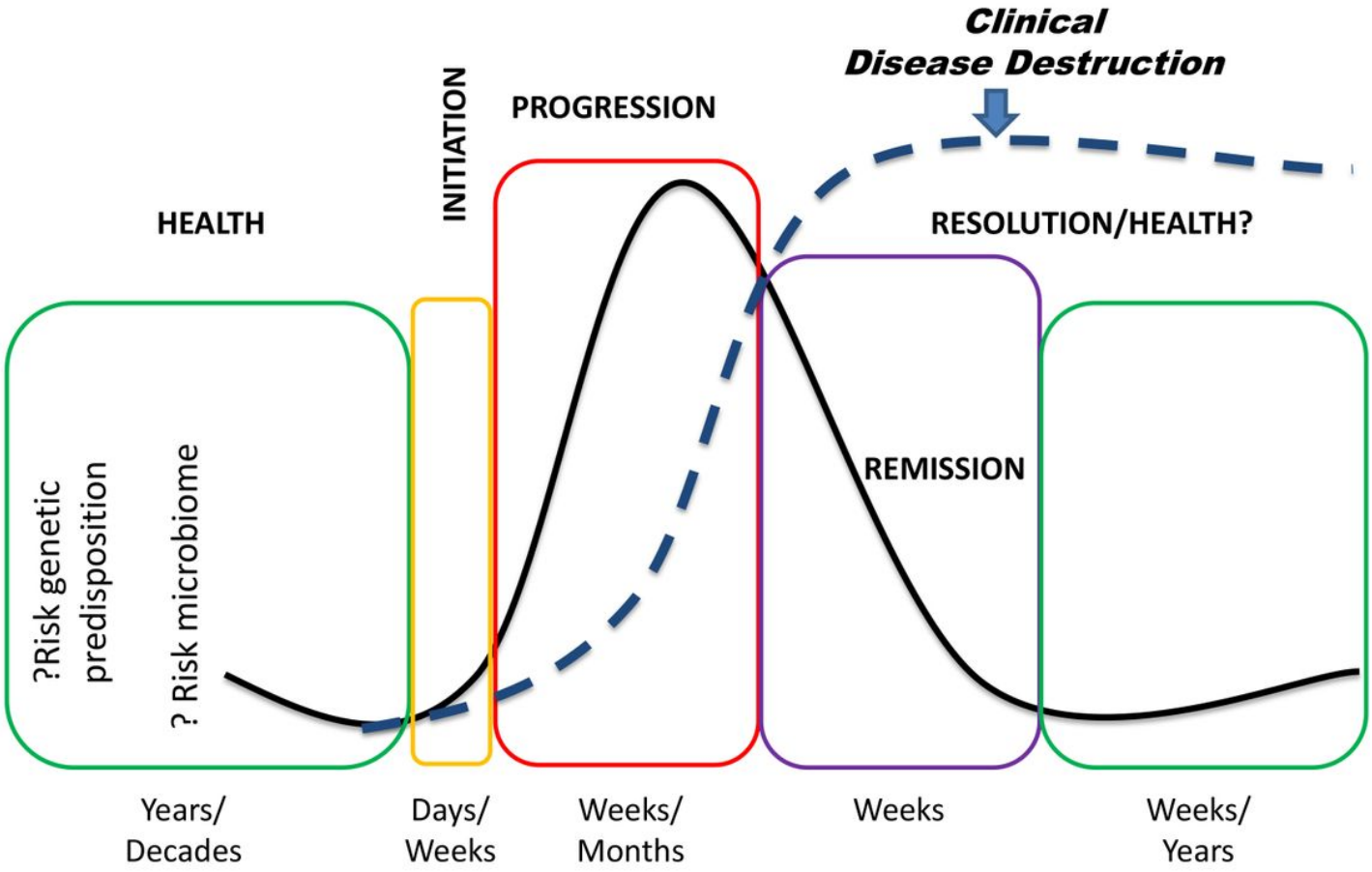

Figure 1

Model of exacerbations and remission of periodontal disease lesions. Graph reflects inherent risk due to genetic predisposition and existing oral microbiome characteristics. Biologic changes occur with initiation and progression of disease the generally presage the clinical changes measured. The model indicates that the biological parameters of disease stabilize and decrease during disease remission and resolution. However, the clinical features of lost epithelial attachment, connective tissue destruction and alveolar bone resorption remain as markers of the previous disease process.

Figure 2

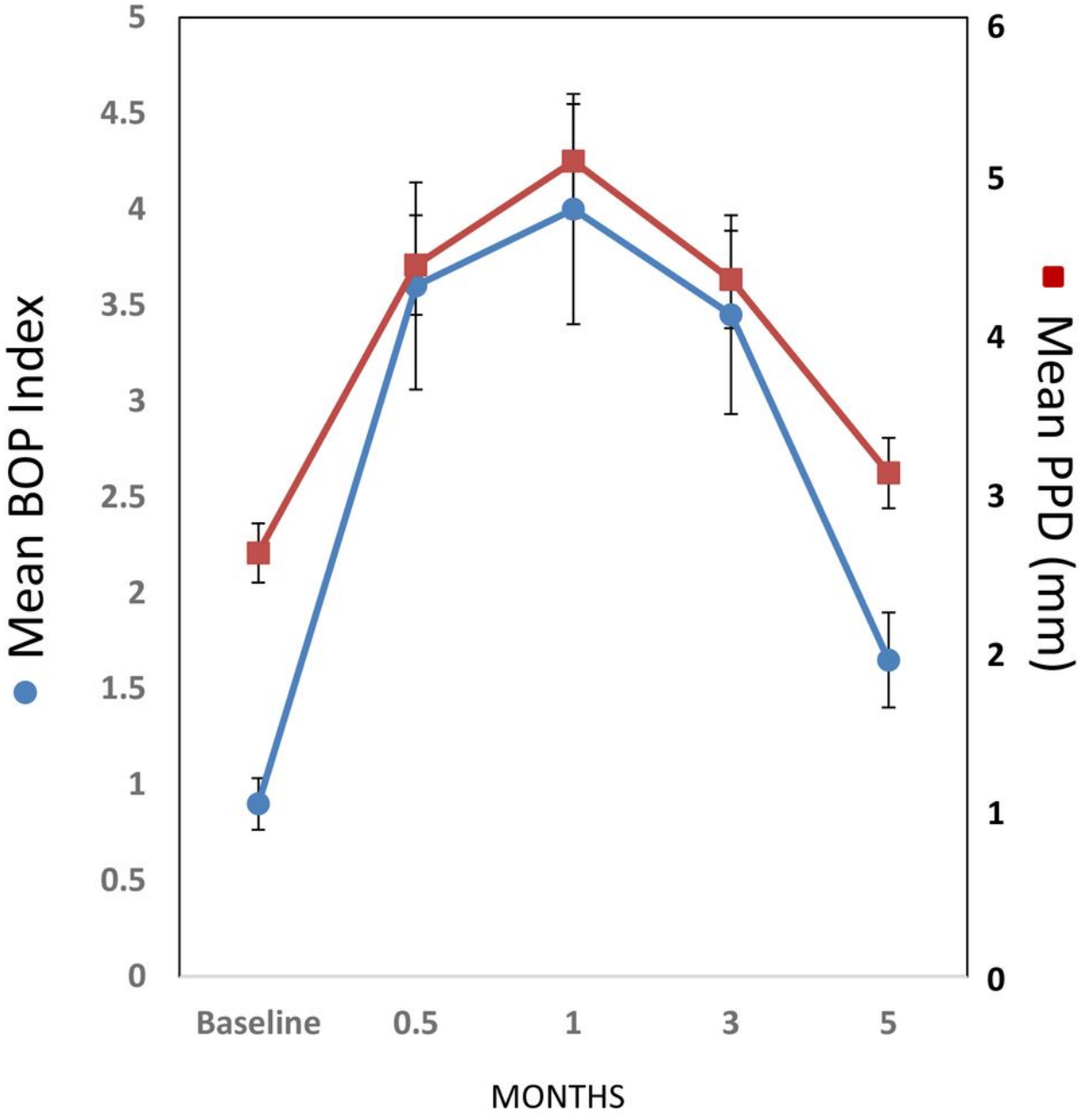

Figure 2

Clinical features of inflammation (bleeding on probing, BOP) and destructive disease (probing pocket depth, PPD) in ligated sites of the nonhuman primates. Ligatures were removed after clinical measures at 3 months, with 5 month samples representing clinical resolution. The points denote the mean values from 18 animals and the vertical brackets enclose 1 SD.

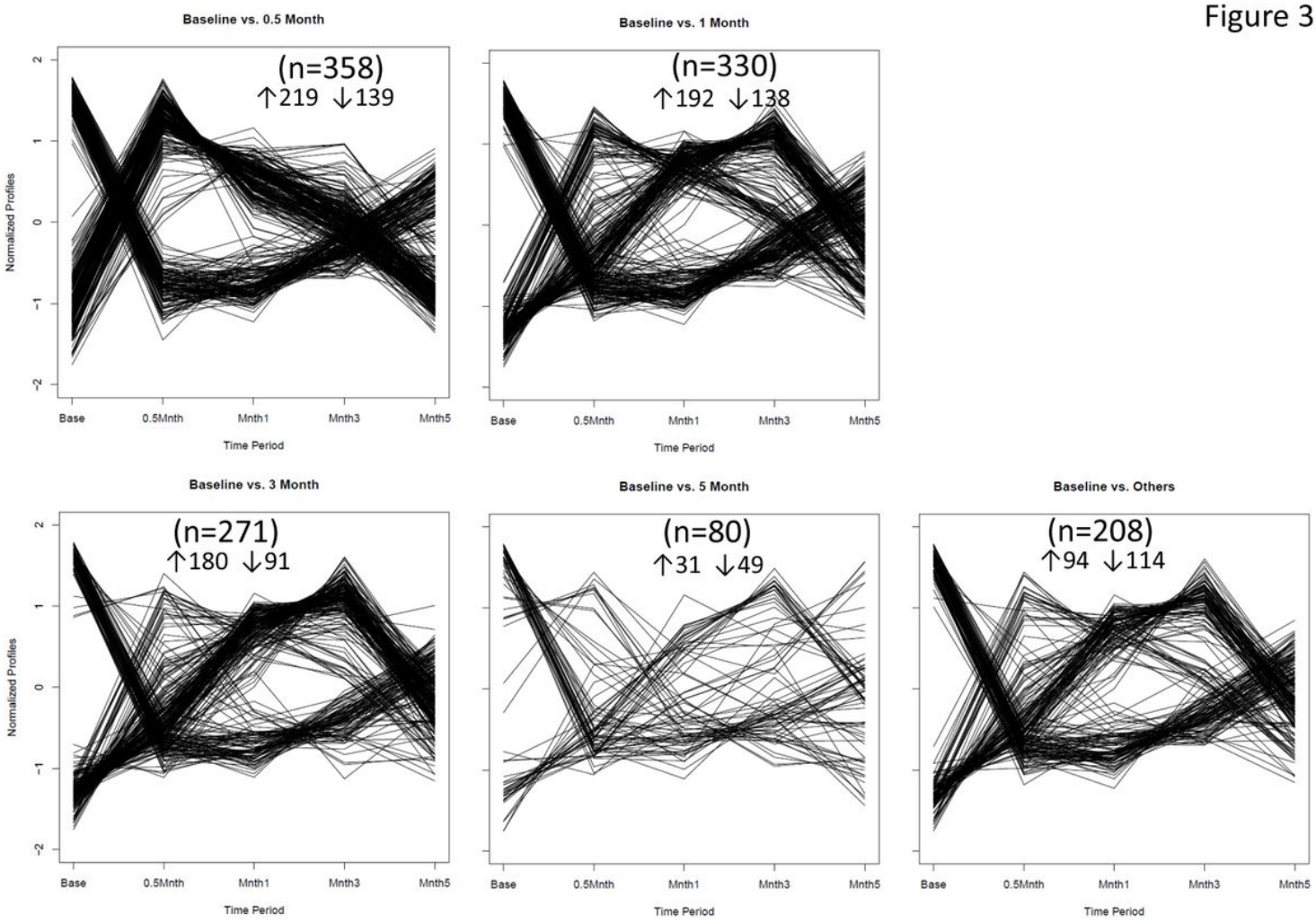

Figure 3

Patterns of gene expression with disease and resolution compared to baseline/health and with each time point of disease or resolution compared to all other time points in the model. Numbers in parentheses denote number of genes within the particular patterns, and whether the patterns denoted up (↑) or down-regulation (↓) of the gene experssion.

Figure 4

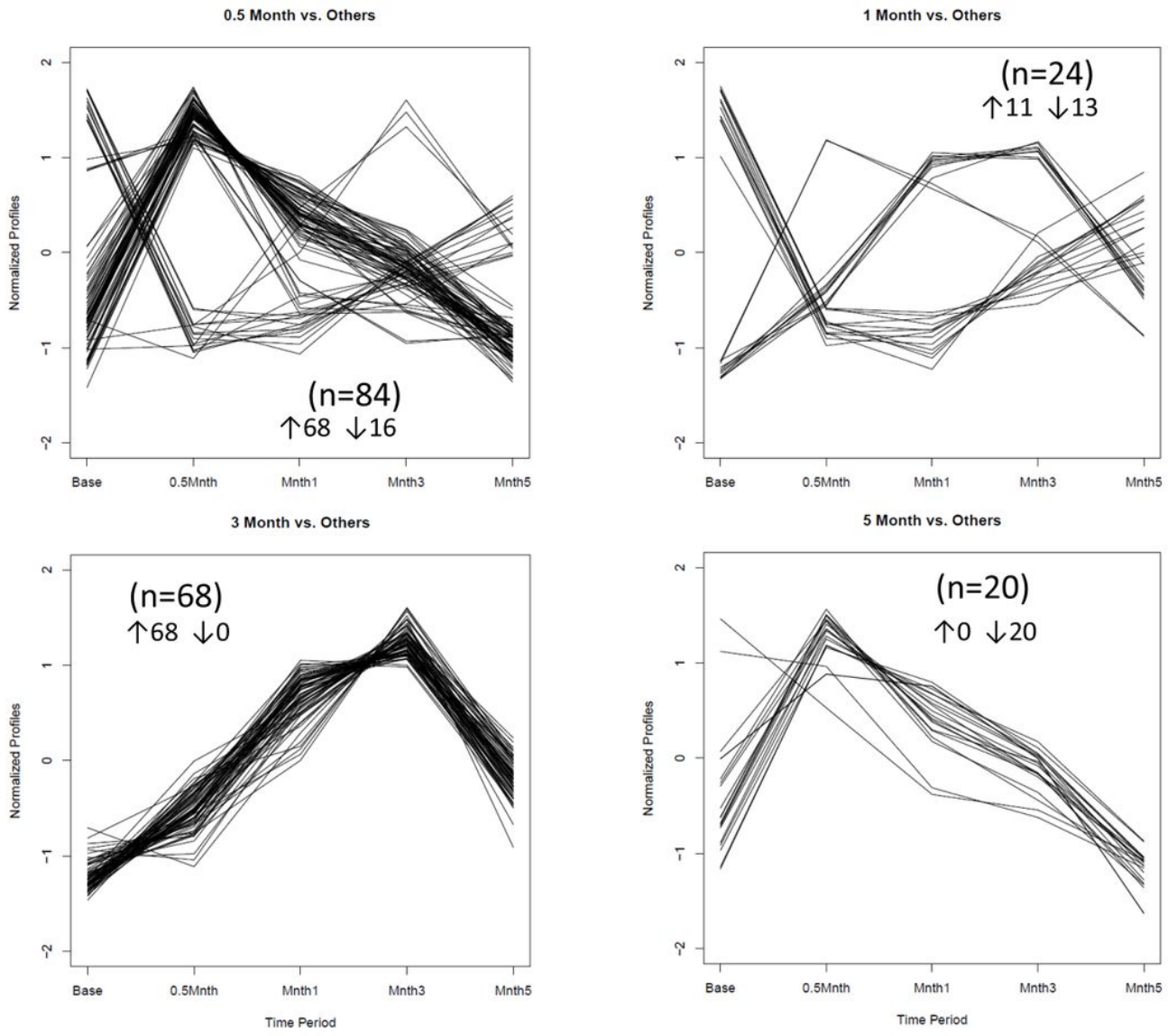

Figure 4

Patterns of gene expression with disease and resolution compared all other time points in the model. Numbers in parentheses denote number of genes within the particular patterns, and whether the patterns denoted up (↑) or down-regulation (↓) of the gene expression.

Figure 5

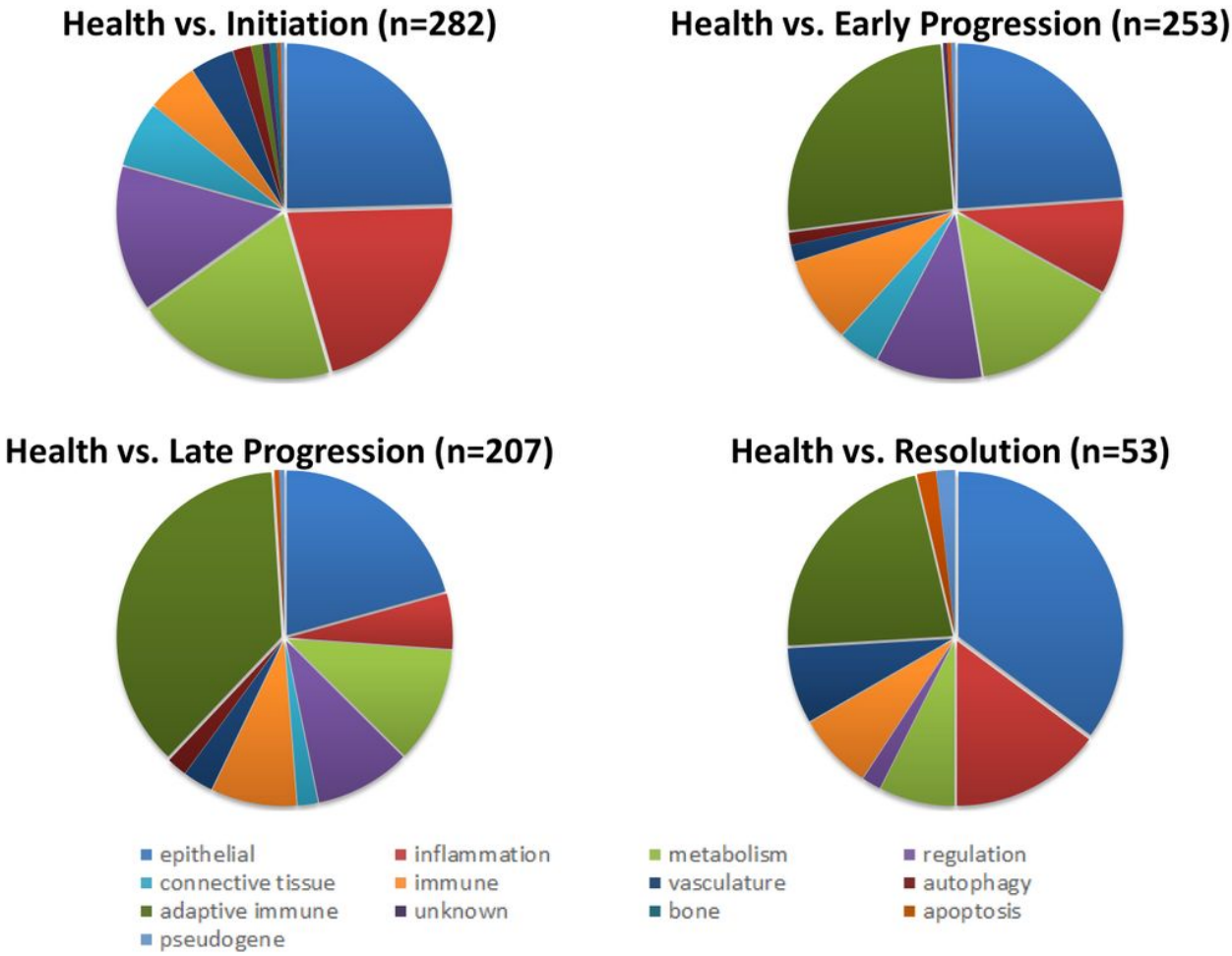

Figure 5

Depiction of the array of genes in various functional categories that differed by ≥ 2-fold at health versus other sampling points. Pie charts denote the proportions of each functional category of genes that comprised the overall number of genes (in parentheses) that were differentially expressed.

Figure 6

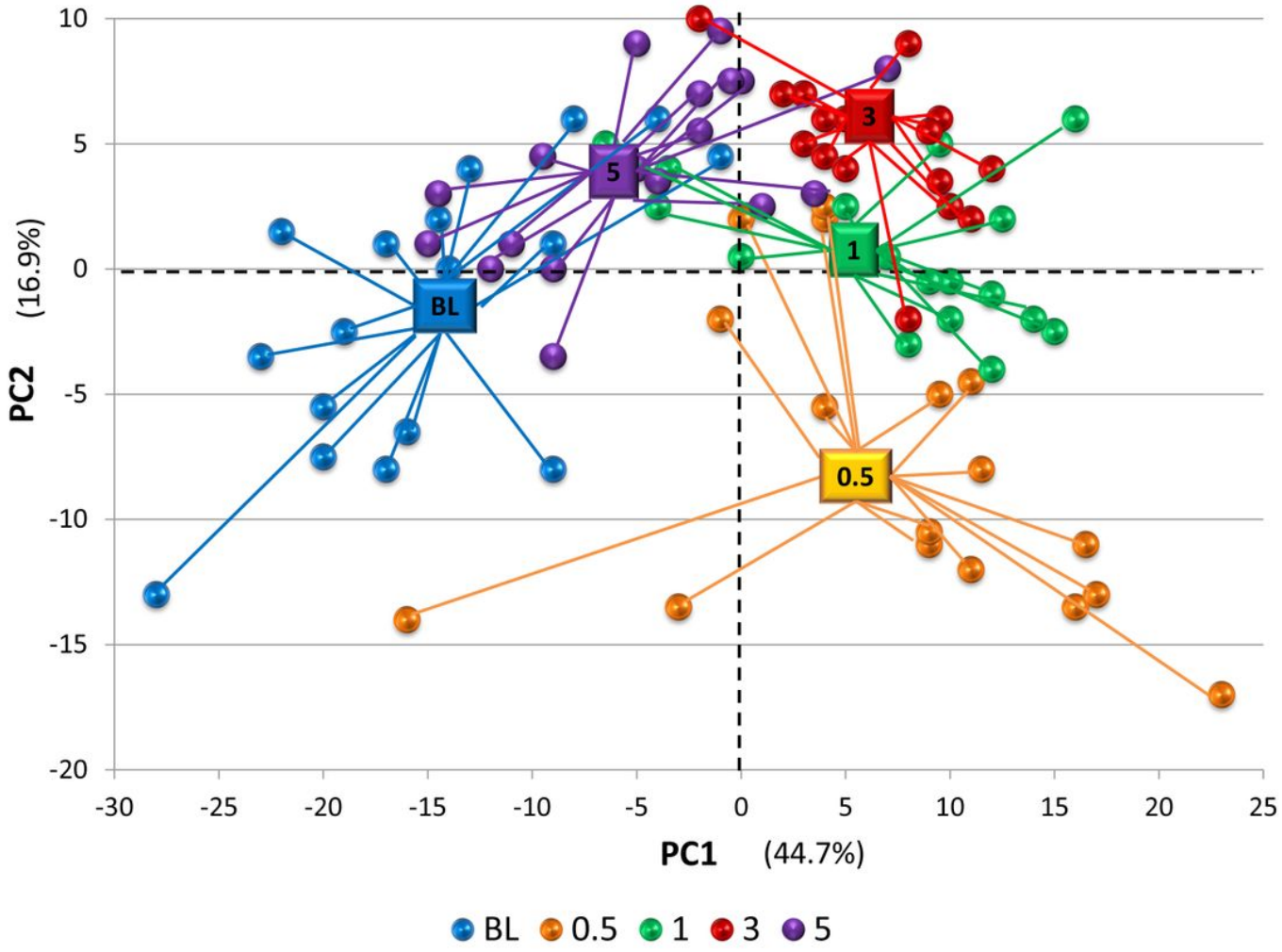

Figure 6

Principal components analysis of the 89 gingival tissue samples using the profile of discriminatory genes identified as disease phase-related. Each point denotes the profile of gene expression for an individual gingival tissue sample collected at baseline (healthy), 0.5 months (initiation), 1 month (early progression), 3 months (late progression), and 5 months (resolution).

Figure 7

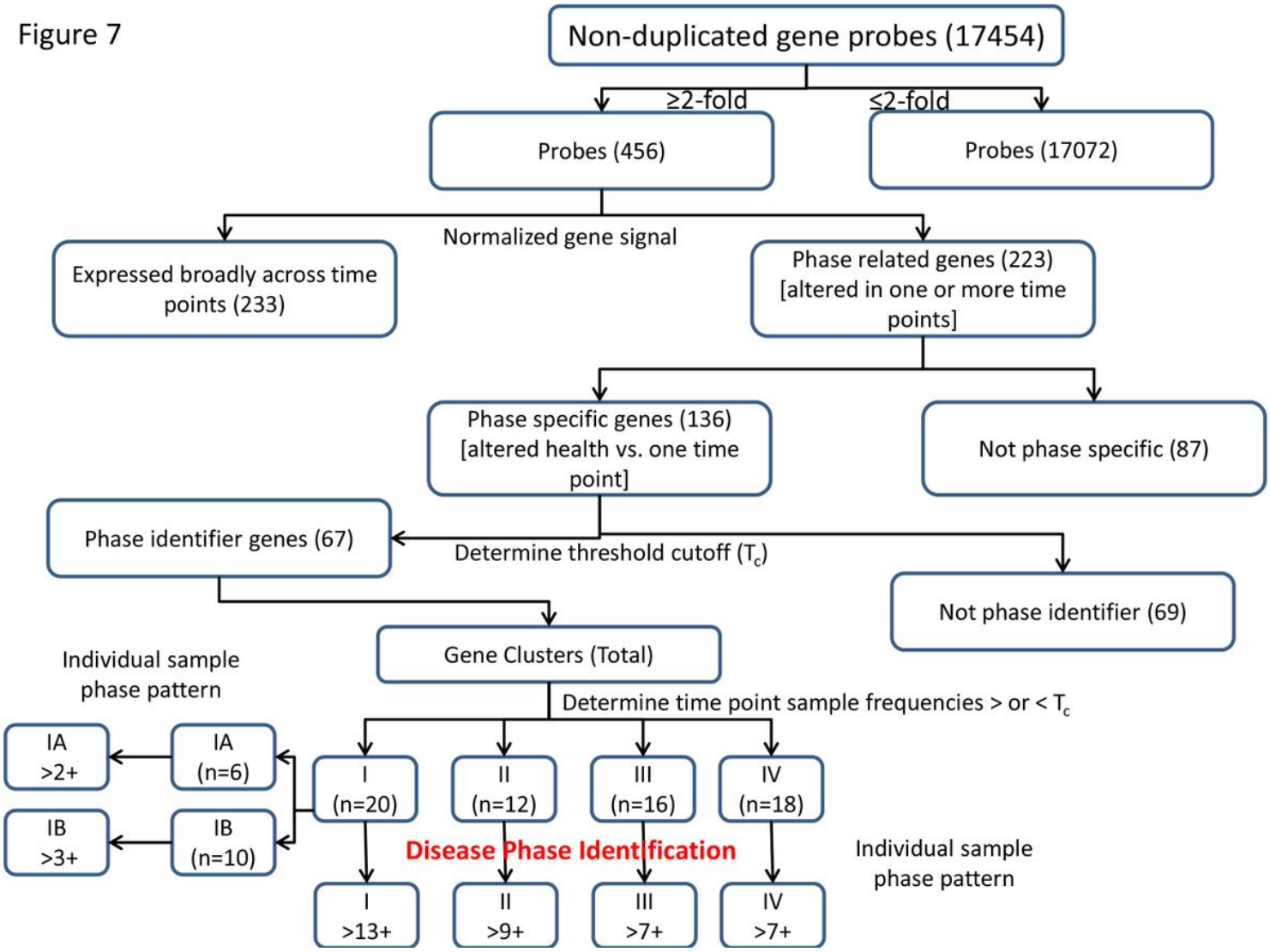

Figure 7

Flow of specific gene selection for discriminating health, phases of disease, and resolution.

Figure 8

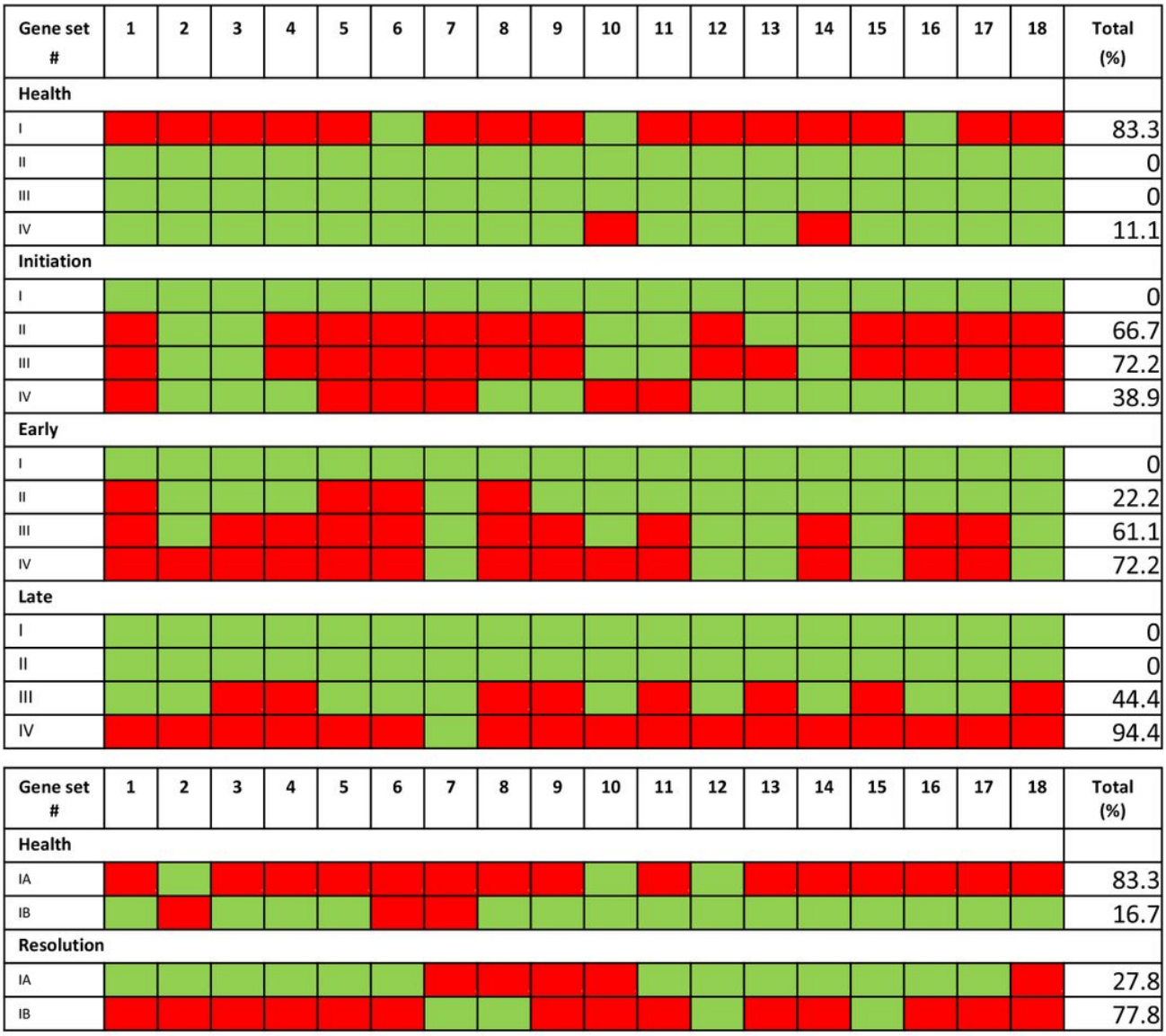

Gene set #	1	2	3	4	5	6	7	8	9	10	11	12	13	14	15	16	17	18	Total (%)
Health																			
I																			83.3
II																			0
III																			0
IV																			11.1
Initiation																			
I																			0
II																			66.7
III																			72.2
IV																			38.9
Early																			
I																			0
II																			22.2
III																			61.1
IV																			72.2
Late																			
I																			0
II																			0
III																			44.4
IV																			94.4

Gene set #	1	2	3	4	5	6	7	8	9	10	11	12	13	14	15	16	17	18	Total (%)
Health																			
IA																			83.3
IB																			16.7
Resolution																			
IA																			27.8
IB																			77.8

Figure 8

Map of response profiles for gene clusters for the 18 samples obtained at each of the timepoints. Red denotes sample demonstrated: Cluster I - >13 genes; Cluster II - >9 genes; Cluster III - >7 genes; Cluster IV - >7 genes with signal greater or less than the threshold cutoff normalized signal (Tc, Table 3). Green denotes sample exhibited fewer genes above or below the Tc. Similar depiction of the distribution of responses to Cluster I genes subgrouped into IA and IB. Red denotes IA - >2 genes and IB - >3 genes above/below the Tc (see Table 3). Total % denotes proportion of the samples that were positive in the gene expression cluster.